Essential Role of Growth Hormone in Ischemia-Induced Retinal Neovascularization

Lois E. H. Smith,* John J. Kopchick, Wen Chen, Joanne Knapp, Fumi Kinose, Douglas Daley, Eliot Foley, Roy G. Smith, James M. Schaeffer

Retinal neovascularization is the major cause of untreatable blindness. The role of growth hormone (GH) in ischemia-associated retinal neovascularization was studied in transgenic mice expressing a GH antagonist gene and in normal mice given an inhibitor of GH secretion (MK678). Retinal neovascularization was inhibited in these mice in inverse proportion to serum levels of GH and a downstream effector, insulin-like growth factor–I (IGF-I). Inhibition was reversed with exogenous IGF-I administration. GH inhibition did not diminish hypoxia-stimulated retinal vascular endothelial growth factor (VEGF) or VEGF receptor expression. These data suggest that systemic inhibition of GH or IGF-I, or both, may have therapeutic potential in preventing some forms of retinopathy.

Neovascularization, the final common pathway in diabetic retinopathy, retinopathy of prematurity, and age-related macular degeneration can cause vision loss. Surgical ablative treatments are incompletely effective and destroy retinal tissue, causing partial visual field loss. Retinal neovascularization remains the most frequent cause of blindness (*1*, *2*).

A role for a pituitary-associated factor in diabetic retinopathy was hypothesized nearly 45 years ago when retinal neovascularization in a diabetic patient was found to regress after pituitary infarction (*3*). For a decade thereafter, many diabetic patients were treated by pituitary ablation. The reduction of retinopathy in these patients appeared to be related to postsurgical GH deficiency, although the role of other pituitary factors could not be eliminated (*4*). GH-deficient dwarfs with glucose intolerance (but without diabetes) have little retinopathy compared to diabetic controls (*5*). Many mitogenic effects of GH are mediated by IGF-I. In some studies of diabetic patients, serum IGF-I levels or vitreal IGF-I levels are associated with proliferative retinopathy (*6*). Clinical trials of early somatostatin (SS) analogs to treat diabetic retinopathy have been inconclusive (*7*).

To investigate the role of the GH–IGF-I –SS axis in ischemia-induced retinal neovascularization and its interaction with VEGF, currently viewed as a major effector of neovascularization (*8–10*), we studied this process in mice with experimentally altered levels of GH. Neovascularization was induced (*11*) in two transgenic mouse lines. The first, G119K, expresses a GH antagonist (Gly^{119} to Lys in bovine GH), which results in a dwarf phenotype. The second line, E117L, expresses a GH agonist (Glu^{117} to Leu in bovine GH) and exhibits a giant phenotype (*12*). There was a 34% decrease in neovascularization (*13*) in GH antagonist mice at postnatal day 17 (P17) compared to nontransgenic littermates ($P \leq 0.0026$) (Table 1). However, transgenic mice expressing the GH agonist E117L had no increase in retinal neovascularization compared to controls (Table 1). As assessed by histologic examination of ocular cross sections, the neovascular response of controls (Fig. 1A) was suppressed in GH antagonist transgenic mice (Fig. 1B). In controls, significant areas of neovascularization were also detected in flat-mounted whole retinas (Fig. 1C) that were perfused with a nondiffusable fluorescein-dextran solution that fills all vessels (*14*). Neovascularization is diminished in GH antagonist G119K retinas (Fig. 1D). No abnormal retinal or vascular development or toxicity was detectable by light microscopy.

We also investigated the effect of MK678, an SS analog that potently inhibits GH release, on retinal neovascularization in nontransgenic mice. MK678 is long-acting and is specific for the SS subtype 2 receptor (*15*). Retinal neovascularization was reduced up to 44% in mice systemically treated with MK678 compared to untreated controls (*16*). The extent of inhibition depended on the MK678 dose (Table 1). In both the G119K transgenic and MK678-treated mice (Table 1), the extent of neovascularization correlated inversely with GH and IGF-I levels (*17*).

The mean serum IGF-I level was 33% less in GH antagonist mice than in controls ($P \leq 0.0001$) and 83% greater in GH agonist mice than in controls ($P \leq 0.027$).

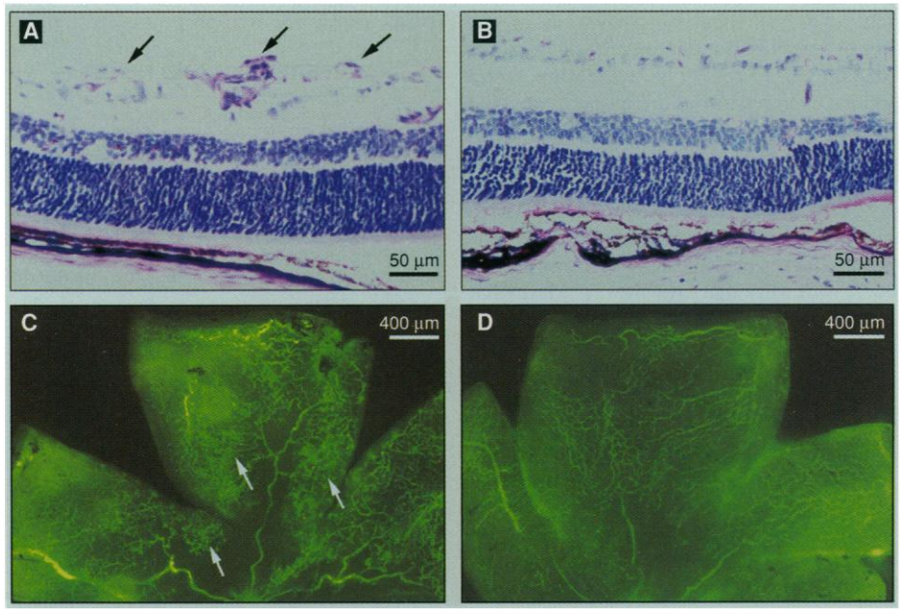

Fig. 1. Effect of GH inhibition on ischemia-induced retinal neovascularization. (**A**) Cross section of an eye from a nontransgenic littermate mouse, showing retinal neovascularization internal to the inner limiting membrane (arrows). (**B**) Cross section of an eye from a GH antagonist G119K transgenic mouse. No vascular cell nuclei are apparent internal to the inner limiting membrane. (**C**) Nontransgenic flat-mounted whole retina, showing extensive areas of retinal neovascularization (*14*) (bright fluorescence, indicated in part with arrows) that is significantly reduced in the retinas from the GH antagonist G119K transgenic mice (**D**).

L. E. H. Smith, F. Kinose, D. Daley, E. Foley, Department of Ophthalmology, Harvard Medical School and Children's Hospital, Boston, MA 02115, USA.
J. J. Kopchick, W. Chen, J. Knapp, Edison Biotechnology Institute, Ohio University, Athens, OH 45701, USA.
R. G. Smith and J. M. Schaeffer, Merck Research Laboratories, Rahway, NJ 07065, USA.

*To whom correspondence should be addressed. E-mail: smith_lo@a1.tch.harvard.edu

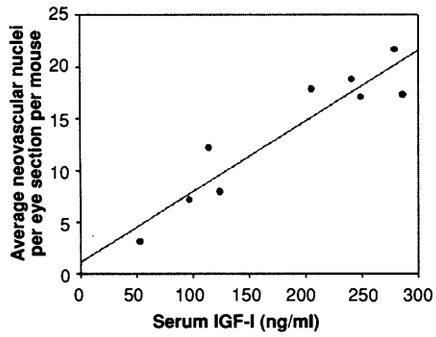

Fig. 2. Linear association between serum IGF-I and retinal neovascularization in mice treated with MK678 (*18*). $y = 0.137x + 2.32$ [y = average number of vascular nuclei per section per mouse, x = serum IGF-I level (ng/ml)], $r^2 = 0.877$, SEE = 4.76, $P < 0.001$.

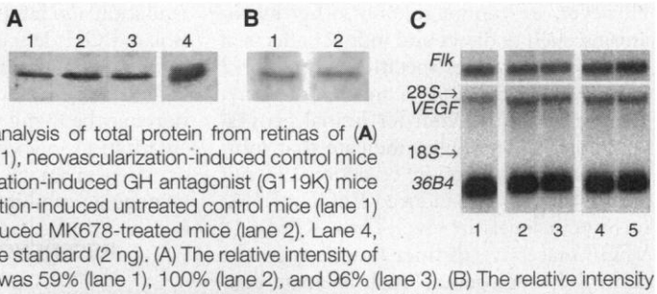

Fig. 3. Immunoblot and Northern analysis of VEGF in retinas from GH-inhibited mice with induced retinal neovascularization. Immunoblot analysis of total protein from retinas of (**A**) room-air control mice (lane 1), neovascularization-induced control mice (lane 2), and neovascularization-induced GH antagonist (G119K) mice (lane 3). (**B**) Neovascularization-induced untreated control mice (lane 1) and neovascularization-induced MK678-treated mice (lane 2). Lane 4, VEGF (23 kD) molecular size standard (2 ng). (A) The relative intensity of lanes normalized to lane 2 was 59% (lane 1), 100% (lane 2), and 96% (lane 3). (B) The relative intensity of lanes normalized to lane 1 was 100% (lane 1) and 105% (lane 2) (*19*). (**C**) Northern blot of total mRNA in GH-inhibited and control retinas, probed for transcripts of *VEGF* [3700 base pairs (bp)], *Flk* (6100 bp), and *36B4* ribozome-associated control (1200 bp). Retinas (at least 22 per lane) were pooled for extraction of total RNA from room-air–exposed normals at P14 (lane 1), neovascularization-induced controls at P14 (lane 2) and P17 (lane 4), and neovascularization-induced MK678-treated mice at P14 (lane 3) and P17 (lane 5). Arrows indicate the ribosomal 28*S* and 18*S* mRNA markers. The relative intensities of *Flk* to *36B4* were 0.18 (lane 1), 0.21 (lane 2), 0.23 (lane 3), 0.19 (lane 4), and 0.30 (lane 5). The relative intensities of *VEGF* to *36B4* were 0.06 (lane 1), 0.13 (lane 2), 0.15 (lane 3), 0.15 (lane 4), and 0.16 (lane 5) (*21*).

Mean serum GH levels from MK678-treated mice declined in proportion to the dose of MK678 (Table 1). IGF-I levels in mice treated with MK678 correlated strongly (*18*) with neovascularization as determined by simple linear regression analysis (Fig. 2).

The role of GH in hypoxia-induced retinal neovascularization was also examined directly by treating MK678-treated mice with exogenous GH. Mice were coinjected subcutaneously with MK678 and murine recombinant GH (mrGH) three times a day to approximate the normal pulsatile release of GH. Even with incomplete restoration of GH, the average number of neovascular nuclei per section per eye was increased from 56% of saline control to 64% of control ($P \leq 0.04$), suggesting that MK678 suppression of retinal neovascularization was mediated at least in part through GH suppression. In parallel studies, retinal neovascularization was induced in mice treated with both MK678 and human recombinant IGF-I (hrIGF-1) (Table 1). Replacement of serum IGF-I completely restored neovascularization to control levels in MK678-treated mice, suggesting that the GH effect was mediated in large part through IGF-I. Exogenous IGF-I alone did not increase neovascularization over control levels (Table 1).

The levels of VEGF, a major stimulus for retinal neovascularization, increase in mouse retina 6 to 12 hours after the onset of hypoxia and remain elevated during the induction of neovascularization. To examine whether the GH/IGF-I effect on neovascularization was mediated directly through VEGF, we evaluated P14 (near maximum *VEGF* mRNA response in this model) and P17 (maximum neovascularization) retinas from MK678-treated or control mice by Northern blot (*19*) for *VEGF* and for VEGF receptor (*Flk-1*) transcripts. In mice with hypoxia-induced retinal neovascularization, neither MK678 treatment nor GH antagonist transgene expression (*20*) inhibited *VEGF* or *Flk* mRNA levels compared to controls at P14 or P17 (Fig. 3C). Immunoblot analysis (*21*) showed no difference in VEGF levels at P17 (Fig. 3A) or P14 (*20*) between transgenic GH antagonist mice (G119K) or controls, nor between MK678-treated and untreated mice at P17 (Fig. 3B) or P14 (*20*). These results suggest that the hypoxia response of VEGF was intact in all models tested.

Our results indicate that inhibition of GH can inhibit ischemia-induced retinal neovascularization in vivo. Neovascularization in animals with inhibited GH secretion was completely restored with exogenous IGF-I. This is consistent with the hypothesis that the inhibition of retinal neovascularization by SS agonists is mediated by a direct lowering of GH levels resulting in a subsequent decrease in IGF-I synthesis.

Table 1. Inhibition of GH in vivo inhibits ischemia-induced retinal neovascularization in mice. Retinal neovascularization was induced in nontransgenic littermate mice (A1) and GH antagonist G119K transgenic mice (A2) (*11*). Eye sections were evaluated for neovascularization (*13*). GH agonist E117L transgenic mice (B4) and nontransgenic littermate controls (B3) were evaluated similarly. C57BL/6 mice (C1 to C7) were evaluated similarly after MK678 treatment (*16*). NS, not significant; ND, not determined.

No.	Mouse	Treatment	*n* (eyes)	Avg. neovascular nuclei per section per eye ± SEM (% of control)	*P**	GH (ng/ml) ± SD (% of control)	IGF-1 (μg/ml) ± SD (% of control)
A1	Control	Nontransgenic	21	23.8 ± 1.7 (100)		0.2 ± 0.03 (100)	93 ± 18 (100)
A2	G119K	Transgenic: GH antagonist	27	15.8 ± 1.8 (66)	<0.003	3.2 ± 0.4 (1590)	62 ± 10 (67)
B3	Control	Nontransgenic	30	18.0 ± 1.6 (100)		0.3 ± 0.02 (100)	76 ± 40 (100)
B4	E117L	Transgenic: GH agonist	29	20.4 ± 1.6 (113)	NS	0.9 ± 0.2 (298)	139 ± 30 (183)
C1	C57BL/6	Saline	35	24.0 ± 0.8 (100)		2.1 ± 2.8 (100)	334 ± 126 (100)
C2	C57BL/6	MK678: 0.06 mg kg^{-1} day^{-1}	21	17.1 ± 0.7 (71)	<0.005	1.2 ± 1.4 (56)	ND
C3	C57BL/6	MK678: 0.6 mg kg^{-1} day^{-1}	18	15.6 ± 0.8 (65)	<0.001	0.9 ± 0.7 (40)	ND
C4	C57BL/6	MK678: 6.0 mg kg^{-1} day^{-1}	16	13.4 ± 0.7 (56)	<0.001	0.13 ± 0.15 (6.1)	234 ± 92 (70)
C5	C57BL/6	MK678: 6.0 mg kg^{-1} day^{-1} +GH: 180 μg kg^{-1} day^{-1}	12	15.4 ± 0.9 (64)	<0.001	0.12 ± 0.25 (5.6)	304 ± 117 (91)
C6	C57BL/6	MK678: 0.6 mg kg^{-1} day^{-1} +IGF-1: 20 mg kg^{-1} day^{-1}	20	23.3 ± 1.4 (97)	NS	ND	377 ± 100 (113)
C7	C57BL/6	IGF-1: 20 mg kg^{-1} day^{-1}	19	23.1 ± 1.2 (96)	NS	ND	367 ± 127 (110)

*With respect to control.

However, we cannot rule out other mechanisms, such as direct and indirect effects of GH and SS analogs specific to receptor 2 (*22*). Although VEGF is an important hypoxia-induced mediator for retinal neovascularization, our studies indicate that inhibition of GH secretion or action did not reduce the hypoxia-induced VEGF mRNA, or protein levels in vivo. Thus, IGF-I and VEGF may have distinct functions in the control of angiogenesis such as acute oxygen regulation (VEGF) versus control of neovascularization on the basis of availability of nutrients for cell division (IGF-I).

No significant increase in neovascularization was observed with the increased GH levels in giant E117L transgenic mice. This observation is in agreement with clinical studies. Patients with overexpression of GH (agromegaly) with or without concomitant diabetes do not have an increased incidence of retinopathy (*23*). There is a linear correlation between serum IGF-I levels and retinal neovascularization in GH-inhibited mice at low and normal serum IGF-I levels (Fig. 2). However, addition of exogenous IGF-I to augment serum levels did not increase retinal neovascularization. These data suggest a permissive role in retinal neovascularization for both GH and IGF-I, with a plateau in response at higher doses. IGF-I receptors are distributed widely in the eye and, although present in vascular cells, they predominate in the neural retina (*24*). Thus, the mechanism of action of IGF-I on the development of retinal neovascularization may be complex and indirect.

In our model of aggressive retinopathy, neovascularization was only partially suppressed by inhibition of GH. Insufficient reduction of GH and serum IGF-I levels or GH-independent local IGF-I production may account for the partial inhibition, as could the possibility that the GH–IGF-I axis is only one of multiple control mechanisms regulating neovascularization. However, the 30 to 44% inhibition of neovascularization that we observed in mice treated with MK678 would be clinically significant. The therapeutic effect is comparable to that observed in the clinical trials that evaluated laser scatter photocoagulation and cryotherapy for diabetic retinopathy and retinopathy of prematurity, respectively (*25*). In this model inhibition of α_v integrins (downstream of VEGF and basic fibroblast growth factor and perhaps other effectors) greatly reduces retinal neovascularization (*26*). Inhibition of either VEGF or GH results in comparable reductions in retinal neovascularization. Inhibition of any one pathway may preferentially affect neovascularization in different pathologic (retinopathy, tumor growth) and beneficial (wound healing, repair of ischemic myocardium, ovulation and fetal development) processes. Isolated GH deficiency in humans appears to allow ovaluation and fetal development (*27*). Thus inhibitors of GH and IGF-I action may be useful for inhibition of neovascularization in specific vascular areas alone or when given in conjunction with other angiogenic inhibitors.

REFERENCES AND NOTES

1. H. A. Klein and H. B. Moorehead, in *U.S. Department of Health, Education and Welfare* (DHEW Publication No. [NIH] 73-427, Bethesda, MD, 1970); Anonymous, *Ophthalmology* **98**, 766 (1991).
2. J. A. McNamara, W. Tasman, G. Brown, *Arch. Ophthalmol.* **110**, 1714 (1992); I. E. Zimmer-Galler, N. M. Bressler, S. B. Bressler, *Int. Ophthalmol. Clin.* **35**, 37 (1995).
3. J. E. Poulsen, *Diabetes* **2**, 7 (1953).
4. A. D. Wright *et al.*, *Br. Med. J.* **ii**, 343 (1969).
5. T. J. Merimee, S. E. Fineberg, V. A. McKusick, *J. Clin. Invest.* **49**, 1096 (1970).
6. T. J. Merimee, J. Zapf, E. R. Froesch, *N. Engl. J. Med.* **309**, 527 (1983); S. A. Amiel *et al.*, *Diabetes* **33**, 1175 (1984); M. B. Grant, B. Russel, C. Fitzgerald, T. J. Merimee, *ibid.* **35**, 416 (1986); S. L. Hyer, P. S. Sharp, R. A. Brooks, J. M. Burrin, E. M. Kohner, *Metabolism* **38**, 5896 (1989); D. G. Dills, S. E. Moss, R. Klein, B. E. Klein, M. Davis, *Diabetes* **39**, 191 (1990); D. G. Dills, S. E. Moss, R. Klein, B. E. Klein, *ibid.* **40**, 1725 (1991); M. Meyer-Schwickerath *et al.*, *J. Clin. Invest.* **92**, 2620 (1993).
7. M. McComb, S. Lightman, D. J. Eckland, A. M. Hamilton, S. L. Lightman, *Eye* **5**, 569 (1991); B. Mallet *et al.*, *Diabete Metabolisme* **18**, 438 (1992); C. Kirkegaard *et al.*, *Acta Endocrinol.* **122**, 766 (1990); S. L. Shumack *et al.*, *Clin. Invest. Med.* **5**, 287 (1990).
8. N. Ferrara, *Eur. J. Cancer* **32A**, 2413 (1996); L. P. Aiello *et al.*, *N. Engl. J. Med.* **331**, 1480 (1994).
9. E. A. Pierce, R. L. Avery, E. D. Foley, L. P. Aiello, L. E. H. Smith, *Proc. Natl. Acad. Sci. U.S.A.* **92**, 905 (1995).
10. G. S. Robinson *et al.*, *ibid.* **93**, 4851 (1996); L. P. Aiello *et al.*, *ibid.* **92**, 10457 (1995).
11. L. E. Smith *et al.*, *Invest. Ophthalmol. Visual Sci.* **35**, 101 (1994). C57Bl/6 mice (P7) were exposed to 75% oxygen, which induces retinal vaso-obliteration. When the mice are returned to room air at P12, VEGF levels increase in the vaso-obliterated hypoxic inner retina (*9*). Extensive retinal neovascularization occurs in 100% of mice by P17. The ischemia-induced retinopathy most closely resembles retinopathy of prematurity. It also has many characteristics of proliferative diabetic retinopathy such as capillary dropout and neovascularizaton of the optic disc. Consequently, this model has been used for efficacy studies for treatment of ischemic retinopathy (*10*, *26*).
12. W. Y. Chen, M. E. White, T. E. Wagner, J. J. Kopchick, *Endocrinology* **129**, 1402 (1991); W. Y. Chen, D. C. Wight, T. E. Wagner, J. J. Kopchick, *Proc. Natl. Acad. Sci. U.S.A.* **87**, 5061 (1990); W. Y. Chen, D. C. Wight, B. V. Mehta, T. E. Wagner, J. J. Kopchick, *Mol. Endocrinol.* **5**, 1845 (1992); W. Y. Chen *et al.*, *J. Biol. Chem.* **266**, 2252 (1991); J. R. Knapp, W. Y. Chen, N. D. Turner, F. M. Byers, J. J. Kopchick, *J. Anim. Sci.* **72**, 2812 (1994). Serum from G119K transgenic mice contained 2.53 μg of the GH antagonist per milliliter and serum from E117L transgenic mice contained 0.55 μg of the GH agonist per milliliter. Serum glucose levels in the G119K, E117L, and control mice showed no significant differences.
13. These studies adhered to the "Association for Research in Vision and Ophthalmology Statement for the Use of Animals in Ophthalmic and Vision Research." Mice were anesthetized with Avertin and killed by intracardiac perfusion of 4% paraformaldehyde in phosphate-buffered saline. The eyes were enucleated and fixed in 4% paraformaldehyde before paraffin embedding. Over 50 serial axial sections (6 μm) were obtained, starting at the optic nerve head. After staining with periodic acid–Schiff reagent and hematoxylin, 10 sections, each 30 μm apart, were evaluated for a span of 300 μm. Eyes with retinal detachment or inflammation (less than 10% of those studied) were excluded. All retinal vascular cell nuclei anterior to the internal limiting membrane were counted in each section in a fully masked protocol. The average number of neovascular cell nuclei per section per eye is the mean of the 10 counted sections. No vascular cell nuclei anterior to the internal limiting membrane were seen in normal unmanipulated animals. The Student's *t* test was used to compare qualitative data populations with normal distributions and equal variance. Data were analyzed with the Mann-Whitney Rank Sum Test for populations with nonnormal distributions or unequal variance.
14. After induction of retinal neovascularization (*11*), eyes were enucleated after intracardiac perfusion with fluorescein-dextran (*28*) in 4% paraformaldehyde. Retinas were isolated, flat-mounted with glycerol-gelatin, and photographed under a fluorescence microscope.
15. K. Raynor *et al.*, *Mol. Pharmacol.* **43**, 838 (1993).
16. Upon induction of hypoxia at P12, mice were injected subcutaneously (10 μl) every 8 hours (until they were killed at P17) with normal saline or with MK678 to achieve 0.06, 0.6, or 6.0 mg kg^{-1} day^{-1} MK678. Some mice were coinjected every 8 hours with MK678 and mrGH to achieve 6.0 mg kg^{-1} day^{-1} MK678 + 180 μg kg^{-1} day^{-1} mrGH (bar 5), or coinjected with rhIGF-I every 6 hours (to achieve 2.0 mg kg^{-1} day^{-1}) + MK678 every 8 hours (to achieve 0.6 mg kg^{-1} day^{-1}) or with rhIGF-I alone every 6 hours (to achieve 2.0 mg kg^{-1} day^{-1}).
17. Serum IGF-I (after acid-ethanol extraction) from at least nine mice for each condition reported was assayed by use of IGF-I radioimmunoassay (RIA) kits (Nichols Institute Diagnostics, San Juan Capistrano, CA) (*12*). Mouse GH was measured by a double-antibody RIA procedure (*12*). GH levels of MK678-treated mice are the means of total serum measurements from at least nine mice obtained from 4 to 6 hours after injection at each condition. All GH and IGF-I errors indicated are standard deviations. Serum levels of GH were increased in GH agonist E117L transgenic mice compared to controls. GH receptor blockage by GH antagonist G119K results in low serum IGF-I levels that serve as a signal for increased production of murine GH (*12*). Therefore murine GH levels were increased in G119K transgenic mice. G119K mice were 34% smaller than controls at P28 because of the GH antagonist effect.
18. In C57Bl/6 mice treated with 6.0 mg kg^{-1} day^{-1} of MK678, serum IGF-I concentration was used as a predictor of change in retinal neovascularization by simple linear regression. The Pearson correlation coefficient, *r*, was used as a measure of linear association. Standard error of the estimate (SEE) was used to indicate error of the regression line. Two-tailed *P* values <0.05 were considered to be statistically significant by use of SPSS software (6.1) (SPSS, Chicago, IL).
19. Twenty micrograms of total RNA from each time point were separated by electrophoresis on formaldehyde-agarose gels and transferred to Biotrans nylon membranes (ICN, Costa Mesa, CA) that were cross-linked with ultraviolet light (Stratalinker 1800, Stratagene). DNA probes were prepared from human *VEGF* cDNA and mouse *Flk* cDNA by random hexamer labeling and [α-^{32}P]deoxycytidine 5′-triphosphate (New England Nuclear, Boston, MA). Autoradiographs were analyzed on a PhosphorImager (Molecular Dynamics) and quantified with ImageQuant PhosphorImager (Molecular Dynamics); *Fms-like tyrosine kinase* (*flt*) mRNA was undetectable on Northern blot under all conditions.
20. L. E. H. Smith, unpublished data.
21. Total retinal protein (at P14 or P17) from 8 to 12 animals for each condition was prepared in SDS sample buffer and resolved by 7.5% SDS–polyacrylamide gel electrophoresis, and 50-μg samples were then transferred to Immobilon-P membranes. Blots were probed with affinity-purified rabbit antibody to mouse VEGF and goat antibody to rabbit immunoglobulin G–horseradish peroxidase (Vector Labs,

Burlingame, CA), visualized with ECL (Amersham, Arlington Heights, IL), and quantified with ImageQuant (Molecular Dynamics).
22. M. B. Grant *et al.*, *Regul. Pept.* **48**, 267 (1993).
23. J. S. Flier and A. C. Moses, in *Endocrinology*, L. J. DeGroot, Ed. (Saunders, Philadelphia, PA, 1989), vol. 2, pp. 1389–1399.
24. C. P. Burren, J. L. Berka, S. R. Edmonson, G. A. Werther, J. A. Batch, *Invest. Ophthalmol. Visual Sci.* **37**, 1459 (1996); P. Moriarty, A. Dickson, D. McCloud, *Br. J. Ophthalmol.* **78**, 638 (1994); I. Jilial, *Endocrinology* **117**, 1222 (1985).
25. The diabetic retinopathy study research group, *Ophthalmology* **88**, 583 (1981); *Arch. Ophthalmol.* **97**, 654 (1979); Cryotherapy for retinopathy of prematurity cooperative group, *ibid.* **108**, 1408 (1990).
26. H. P. Hammes, M. Brownlee, A. Jonczyk, A. Sutter, *Nature Med.* **2**, 529 (1996).
27. Z. Laron, R. Sarel, A. Pertzelan, *Eur. J. Pediatrics* **134**, 79 (1980).
28. R. D'Amato, E. Wesolowski, L. E. Smith, *Microvasc. Res.* **46**, 135 (1993).
29. We thank X. Xu, R. Sullivan, T. Meehan, R. Webb, K. Cheng, T. W. Wu, and S. Satiritz for assistance and D. Senger and K. Claffey for helpful discussions. Supported in part by grants from the V. Kann Rasmussen Foundation and the National Eye Institute (EY08670 to L.E.H.S.) and the Ohio State Eminent Scholars Program, Sensus Corporation, and the Juvenile Diabetes International (195061 to J.J.K.).

10 February 1997; accepted 14 May 1997

Regulation of Mitochondrial Iron Accumulation by Yfh1p, a Putative Homolog of Frataxin

Michael Babcock, Deepika de Silva, Robert Oaks, Sandra Davis-Kaplan, Sarn Jiralerspong, Laura Montermini, Massimo Pandolfo, Jerry Kaplan*

The gene responsible for Friedreich's ataxia, a disease characterized by neurodegeneration and cardiomyopathy, has recently been cloned and its product designated frataxin. A gene in *Saccharomyces cerevisiae* was characterized whose predicted protein product has high sequence similarity to the human frataxin protein. The yeast gene (yeast frataxin homolog, *YFH1*) encodes a mitochondrial protein involved in iron homeostasis and respiratory function. Human frataxin also was shown to be a mitochondrial protein. Characterizing the mechanism by which *YFH1* regulates iron homeostasis in yeast may help to define the pathologic process leading to cell damage in Friedreich's ataxia.

Friedreich's ataxia (FRDA) is an autosomal recessive degenerative disease characterized by progressive gait and limb ataxia, signs of axonal sensory neuropathy, pyramidal weakness of the legs, and dysarthria (*1*). A hypertrophic cardiomyopathy is found in almost all affected individuals (*1*, *2*). Diabetes mellitus accompanied by a loss of pancreatic β cells is seen in about 10% of the cases, carbohydrate intolerance is present in an additional 20%, and all patients show abnormal insulin secretion in response to amino acid stimulation (*3*).

The molecular defect in FRDA was identified as a deficiency of frataxin, a small protein (210 amino acids) whose function could not be identified by amino acid sequence analysis (*4*). Frataxin deficiency may occasionally be traced to nonsense, splice site, or missense point mutations, but the primary cause is the hyperexpansion of a polymorphic GAA trinucleotide repeat situated in the first intron of the corresponding gene, which results in a marked reduction in the steady-state level of mature frataxin mRNA (*4*, *5*). RNA analysis of frataxin expression in adult human tissues (*4*) and in situ hybridization studies in the mouse (*6*) suggested a direct correlation between the pattern of degeneration observed in the disease and the sites of frataxin transcription, which is highest in heart, spinal cord, and dorsal root ganglia. A recent study proposed that frataxin was encoded in a larger transcriptional unit than originally thought, and that its gene was in fact part of the neighboring *STM7* gene, which was transcribed in the same direction and encoded a phosphatidylinositol 4-phosphate 5-kinase (*7*). New evidence suggests that the inclusion of *STM7* sequence as part of the FRDA gene was based on polymerase chain reaction (PCR) conditions that amplified rare and illegitimate transcripts not usually detected in vivo (*5*). All of the FRDA mutations identified to date are located in the original 3′ "frataxin" region of the gene (*4*, *5*).

Genes encoding predicted proteins with high sequence similarity to frataxin have been identified in mouse, rat, *Caenorhabditis elegans*, and an anonymous open reading frame (YDL120w) in *Saccharomyces cerevisiae* (*6*, *8*). The predicted yeast frataxin homolog was independently identified as a multicopy suppressor of a mutant (*bm-8*) that was unable to grow on iron-limited medium. The *bm-8* mutant was transformed with a genomic library, and a clone was identified that partially overcame the low-iron growth deficit (*9*). The region responsible for the complementing activity was identified by subcloning the open reading frame YDL120w on chromosome IV (*10*). BLAST analysis of this sequence identified two proteins with high sequence similarity, the predicted product of an anonymous open reading frame in the *C. elegans* genome and human frataxin. We determined that *YFH1* was not allelic to *bm-8*. First, no complementation was seen when *bm-8* was transformed with *YFH1* on a centromeric plasmid. Second, allelic segregation demonstrated that a *LEU2* marker integrated next to the chromosomal copy of *YFH1* segregated away from *bm-8* (*11*). Third, the gene allelic to *bm-8* was cloned by genomic complementation and the open reading frame (YMR134w) localized to chromosome XIII. Although these results demonstrate that *YFH1* was not responsible for the phenotype of *bm-8*, the fact that overexpression of *YFH1* alleviated the *bm-8* low-iron growth defect suggested that it was involved in iron metabolism.

To define the function of *YFH1*, we disrupted the chromosomal copy by inserting the *HIS3* auxotrophic marker into the open reading frame (*12*). Disruptants were selected and deletion of *YFH1* confirmed by Southern (DNA) analysis. The Δ*yfh1* (*yfh1*::*HIS3*) strain showed a severe growth deficit on fermentable carbon sources regardless of iron concentration. The deletion strain was unable to grow on rich medium containing glycerol and ethanol (YPGE) as the carbon source, suggesting that Δ*yfh1* was unable to carry out oxidative phosphorylation. The disruptant was also unable to grow on any media at 37°C. The respiratory incompetence of Δ*yfh1* was confirmed by demonstrating a severe reduction in oxygen consumption, even in cells grown in rich medium (*13*). We hypothesized that the Δ*yfh1* cells were unable to grow on fermentable carbon sources as a result of the generation of *rho*$^-$ mutants. These *rho*$^-$ mutations are characterized by defects in or loss of mitochondrial DNA and an inability to carry out oxidative phosphorylation. Lack of growth on respiratory substrates in Δ*yfh1* was shown to be the result of a loss of mitochondrial DNA. Diploids generated from a cross between Δ*yfh1* and wild-type cells were respiratory competent, whereas diploids from Δ*yfh1* and a *rho* tester strain (*rho*^{0}) were unable to grow on

M. Babcock, D. de Silva, R. Oaks, S. Davis-Kaplan, J. Kaplan, Division of Immunology and Cell Biology, Department of Pathology, School of Medicine, University of Utah, Salt Lake City, UT 84132, USA.
S. Jiralerspong and L. Montermini, Centre de Recherche Louis-Charles Simard, Montréal, Québec, H2L4M1 Canada.
M. Pandolfo, Department of Medicine, Université de Montréal, Montréal, Québec, H2L4M1 Canada, and Department of Neurology and Neurosurgery, McGill University, Montréal, Québec, H3A2B4 Canada.
*To whom correspondence should be addressed.